Localized surface phonon polariton resonances in polar gallium nitride

Kaijun Feng,[1,a)] William Streyer,[2] S. M. Islam,[1] Jai Verma,[1] Debdeep Jena,[1,3] Daniel Wasserman,[2] and Anthony J. Hoffman[1]
[1]*Department of Electrical Engineering, University of Notre Dame, Notre Dame, Indiana 46556, USA*
[2]*Department of Electrical and Computer Engineering, University of Illinois Urbana-Champaign, Urbana, Illinois 61801, USA*
[3]*School of Electrical and Computer Engineering, Cornell University, Ithaca, New York 14850, USA*

(Received 20 May 2015; accepted 13 August 2015; published online 24 August 2015)

We demonstrate the excitation of localized surface phonon polaritons in an array of sub-diffraction pucks fabricated in an epitaxial layer of gallium nitride (GaN) on a silicon carbide (SiC) substrate. The array is characterized via polarization- and angle-dependent reflection spectroscopy in the mid-infrared, and coupling to several localized modes is observed in the GaN *Reststrahlen* band (13.4–18.0 μm). The same structure is simulated using finite element methods and the charge density of the modes are studied; transverse dipole modes are identified for the transverse electric and magnetic polarizations and a quadrupole mode is identified for the transverse magnetic polarization. The measured mid-infrared spectrum agrees well with numerically simulated spectra. This work could enable optoelectronic structures and devices that support surface modes at mid- and far-infrared wavelengths. © *2015 AIP Publishing LLC*. [http://dx.doi.org/10.1063/1.4929502]

A pillar of nanophotonics is the interaction of light with collective charge oscillations using free electrons and holes—a field known as plasmonics. These charge oscillations, called plasmons, typically comprise free electrons in a metal or semiconductor. Around the plasmon frequency, which is determined primarily by charge density and electron effective mass, the optical properties of the plasmonic material change rapidly. At frequencies lower than the plasmon resonance frequency, the permittivity is negative. A negative permittivity enables devices and structures that exhibit extraordinary behavior such as sub-diffraction mode confinement and field enhancement.[1–3] These devices and structures have potential applications in a variety of fields, including sensing and photonic circuits.[4,5] Despite immense interest and potential, the application of plasmonic devices is usually limited by significant optical loss.

A principal concern with plasmonic materials is the large inherent loss due to scattering of free electrons.[6] Metals such as silver are the conventional choice in the visible to near ultraviolet (UV) region, and plasmon lifetimes are typically on the order of tens of femtoseconds (fs).[7] For longer wavelengths in the near-infrared (near-IR) to mid-infrared (mid-IR), doped semiconductors can be used as plasmonic materials.[8,9] The optically excited carrier scattering time in semiconductors is on the order of 100 fs.[10] Despite the improvements, the loss is still significant and further improvements are desirable. Recent efforts have focused on improving plasmonic loss via a number of strategies, including developing novel materials such as transparent conductive oxide (TCO)[11] and introducing gain into the system.[12]

In the long wavelength mid-IR and far-infrared (far-IR), an alternative approach to plasmonics exists using polar dielectric crystals: instead of coupling to collective oscillations of free-carriers, light couples to coherent oscillations of the polar lattice (optical phonons). At frequencies between the transverse optical (TO) phonon and longitudinal optical (LO) phonon frequencies, which is referred to as the *Reststrahlen* band, the permittivity of the material is negative.[13] Additionally, natural hyperbolic materials, resulting from strong anisotropy of the crystal, have been demonstrated in hexagonal boron nitride.[14,15] Similar to plasmonic materials, polar crystals can support optical modes that are confined to the surface of the material. These surface phonon polaritons (SPhP) can be excited using techniques similar to their plasmonic counterparts, surface plasmon polaritons (SPP).[13,16] Likewise, the SPhPs can also be highly confined within (or in the vicinity of) sub-diffraction geometries, resulting in strong field enhancement.[17,18] These confined SPhP modes are generally referred to as localized SPhPs.[19–22] Compared to plasmonic materials, the phononic materials typically exhibit a smaller imaginary part of the permittivity at identical values of the real part, which is advantageous for realizing high Q resonances.[23]

In this work, we design and fabricate sub-diffraction optical resonators using the polar semiconductor gallium nitride (GaN). GaN is a wide bandgap (3.4 eV) semiconductor, which has been widely used in modern electronic and photonic devices.[24,25] GaN and other III-nitride heterostructures can be grown using epitaxial techniques such as molecular beam epitaxy (MBE), hydride vapor phase epitaxy (HVPE), and metal-organic chemical vapor deposition (MOCVD).[26] These growth techniques allow precise control over material layer thicknesses and enable the development of myriad devices; III-nitride light emitting diodes (LED)[27] and laser diodes (LD)[28] are now able to cover the blue part of the visible, as well as the ultraviolet, spectra. The established growth and mature fabrication technologies make GaN an attractive material choice for phonon polariton devices as these previous advances can be leveraged to develop more sophisticated devices that could enable new

[a)]Author to whom correspondence should be addressed. Electronic mail: kfeng@nd.edu

optoelectronic devices for the mid-IR. The substrate type and orientation used for growth influence the optoelectronic properties of the epitaxial GaN, and more than six different materials can be used as substrates.[29] The flexibility in the choice of the substrate enables both hetero- and homo-epitaxial growth of GaN and enables a larger optical design space. Among the various substrates, sapphire (Al_2O_3) and SiC are the most common.[24] GaN grown on (0001) Al_2O_3 or 6H-SiC is polar due to spontaneous and piezoelectric induced polarization.[30–32] In this research, 670 nm of intrinsic GaN was grown on 6H-SiC substrate using plasma assisted MBE.

In the mid-IR portion of the spectrum, the permittivity of GaN is determined primarily by optical phonon energies and the free-carrier concentration, which can be controlled via impurity doping. In general, the permittivity for both GaN and SiC are anisotropic; however, isotropic models reduce the complexity of calculations and are good approximations in most applications.[19,21] Since both the GaN epitaxial layer and the SiC substrate used in this program have low free-carrier concentrations, the contribution to the permittivity from free-carriers is ignored for both materials in this work. The contribution to the permittivity of a polar semiconductor from optical phonons is modeled using a Lorentzian function[33]

$$\varepsilon = \varepsilon_\infty \left(1 + \frac{\omega_{LO}^2 - \omega_{TO}^2}{\omega_{TO}^2 - \omega^2 + i\omega\Gamma}\right). \quad (1)$$

Here, ω_{LO} is the longitudinal optical (LO) phonon frequency, ω_{TO} is the transverse optical (TO) phonon frequency, and Γ is a damping constant related to the optical phonon lifetime. When the frequency of light is between the TO and LO frequencies (the *Reststrahlen* band), the permittivity is negative. At the LO phonon frequency, the material permittivity crosses from positive to negative, such that $\varepsilon(\omega_{LO}) \sim 0$.

We use Eq. (1) to model the permittivity of the polar GaN layer and SiC substrate. We characterized the reflectivity of the bare GaN/SiC sample at mid-infrared wavelengths using a Bruker Vertex 80v Fourier Transform infrared (FTIR) vacuum spectrometer with an internal room-temperature DLaTGS detector. The angle-dependent reflectivity was measured under vacuum using a PIKE Technologies VeeMAX III specular reflectance accessory. An isotropic transfer matrix model was used with Γ_{GaN} (damping constant for GaN) and the TO and LO phonon energies as fitting parameters. The damping constant was calculated as 9 cm^{-1}, and the TO and LO phonons have frequencies of 556 and 735 cm^{-1}, respectively. All of these values are in good agreement with other published results.[33–35] The phonon frequencies for the SiC substrate were taken from literature:[36] $\omega_{TO} = 797\,cm^{-1}$ and $\omega_{LO} = 970\,cm^{-1}$. The damping constant for SiC was determined as 5 cm^{-1} via fitting to the experimental data. Fig. 1(a) depicts the real and imaginary parts of the isotropic permittivity for intrinsic GaN and SiC using the specified parameters. An important feature of the GaN-SiC material system is that the SiC substrate behaves as a dielectric—albeit a lossy dielectric—in the GaN *Reststrahlen* band because the TO and LO phonon

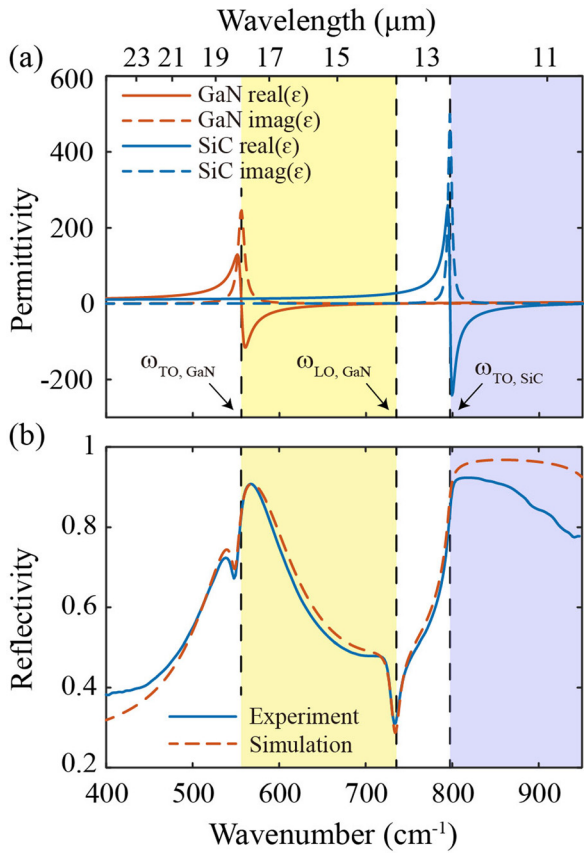

FIG. 1. (a) Permittivity of GaN and SiC. $\omega_{TO,GaN} = 556\,cm^{-1}$, $\omega_{LO,GaN} = 735\,cm^{-1}$, $\omega_{TO,SiC} = 797\,cm^{-1}$, and $\omega_{LO,SiC} = 970\,cm^{-1}$. The *Reststrahlen* bands of GaN and SiC are shaded yellow and blue, respectively. (b) Experiment and simulation result of the reflectivity of GaN thin film on SiC substrate, with the *Reststrahlen* bands shaded as in Fig. 1(a). The incident angle is 30°.

frequencies for SiC have higher energies. For example, at $\omega = 650\,cm^{-1}$(in the middle of the *Reststrahlen* band of GaN), $\varepsilon_{SiC} = 16.0 + 0.1i$; based on a simple calculation we have the attenuation coefficient $\alpha = 73\,cm^{-1}$. Compared to approaches using different polar materials, the SiC substrate is attractive because it enables strong confinement of light within the GaN structures due to a large index contrast; also the relatively low loss of SiC can result in longer propagation length. A comparison between the measurement and transfer matrix calculations is shown in Fig. 1(b) for an incident angle of 30°. The agreement within the *Reststrahlen* band of GaN (shaded yellow region) is excellent. The deviation between experiment and calculations in the SiC *Reststrahlen* band (shaded blue region) may be due to the presence of background doping or a native oxide.[37]

A 0.5 × 0.5 cm^2 array of GaN pucks with a diameter of 3.2 μm and a period of 4.8 μm were fabricated using standard processing techniques. A nickel etch mask was created using photolithography and electron beam evaporation. The pucks were etched the entire thickness of the GaN epitaxial layer using an inductively coupled plasma reactive ion etch (ICP-RIE). Finally, the nickel mask was removed using a HF and HNO_3 wet etch. Fig. 2(a) shows an image of the fabricated array obtained using tilted scanning electron microscopy. Over the entire fabricated area, the uniformity of the puck diameter is excellent except for sparse fabrication defects.

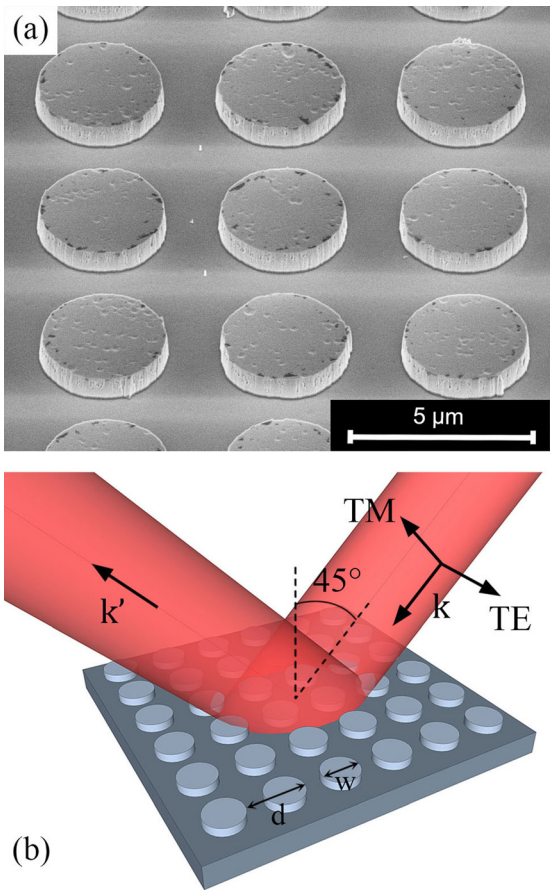

FIG. 2. (a) SEM picture of the fabricated GaN micro-disk array with pitch d = 4.8 μm and diameter w = 3.2 μm. (b) Schematic of the reflection of fabricated GaN sample. The image is not to scale because the real beam spot is much larger than a single disk.

The fabricated puck arrays were spectrally characterized using FTIR spectroscopy. Polarization-dependent reflection spectra were measured for incident angles from 40° to 60°. using a KRS-5 holographic wire grid polarizer. The samples were characterized in the FTIR sample compartment and all spectral measurements were performed under vacuum. Fig. 2(b) is a schematic of the incident and reflected beam for an incident angle of 45°, and the direction of the electric field for the transverse magnetic (TM) and transverse electric (TE) polarizations used in the measurements. The measurement results for the TM and TE light are shown in Figs. 3(a) and 3(b), respectively. For each measurement, the reflection spectra were normalized to the spectrum of a gold-coated mirror at the same incident angle and with the same polarization of the incident light. Several dips in the spectra are present and indicate coupling to localized SPhP modes.

To confirm the presence of these localized modes, we used the commercial finite element analysis (FEA) software COMSOL Multiphysics with a full 3D model to simulate the reflectivity of the micro-puck array based on the isotropic dielectric model of GaN and SiC shown in Fig. 1(a). The TM and TE simulated reflectivity for 45° are shown in Fig. 4(a) as dashed lines and compared to the measured spectra (solid lines). There is strong agreement between experiment and simulation, except for a discrepancy around 680 cm^{-1}, where the simulation predicts two resolved TM modes while the modes are much closer in the experiment.

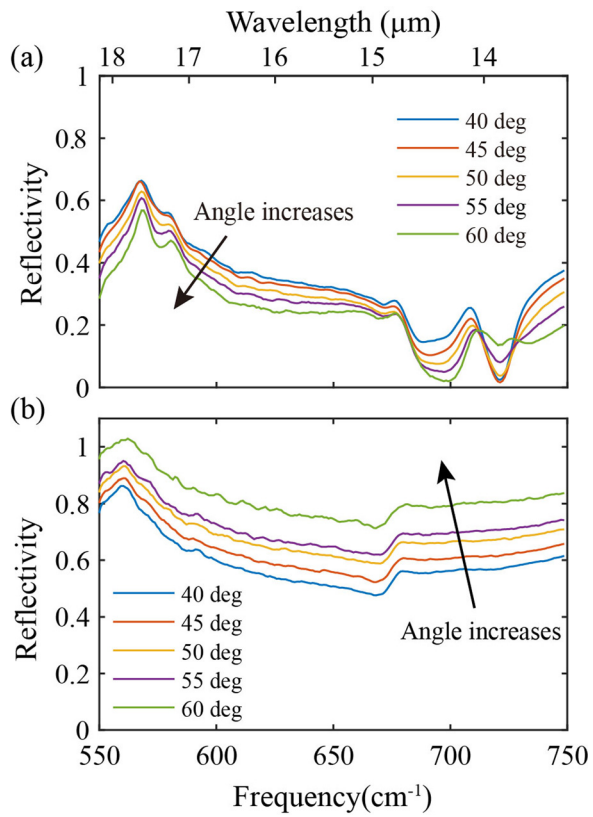

FIG. 3. (a) TM reflection spectra of the micro-puck array with different incident angles. (b) TE reflection spectra of the micro-puck array with different incident angles.

This discrepancy may be due to surface damage and residual chlorine from the RIE process,[21] which can broaden the modes, and differences in the experimental and simulated shapes and permittivities, which influences the separation between the modes.

The numerical simulations can be used to further understand the nature of the localized modes. The shapes of the absorption valleys in Fig. 4(a) reveal the quality factors of the oscillation modes at the corresponding frequencies, which is in the range of 10–60. The charge density of 4 representative modes are depicted in Fig. 4(b). For these images, the charge density was calculated using Gauss's law and normalized to a constant value. The charge distribution for TE modes (i) and (ii), also indicated on Fig. 4(a), show that these localized modes correspond to transverse dipoles. The frequency difference is primarily determined by the different media surrounding the GaN puck, which can be roughly estimated as[17]

$$Re[\varepsilon(\omega)] = -2\varepsilon_m, \tag{2}$$

where $\varepsilon(\omega)$ is the permittivity of the material of the nanostructure, i.e., GaN in this case. ε_m is the permittivity of the surrounding media, which are air and SiC for the two modes, respectively. Using air and SiC as surrounding media, Eq. (2) leads to two localized modes frequencies at 589 and 691 cm^{-1}, respectively. As is shown in Fig. 4, mode (i) at the base of the puck is close to the former frequency for SiC; modes (ii), (iii), and (iv), which are on the top of the puck are close to the second frequency for air. For TM light, the two modes with the strongest coupling are (iii) and (iv). TM

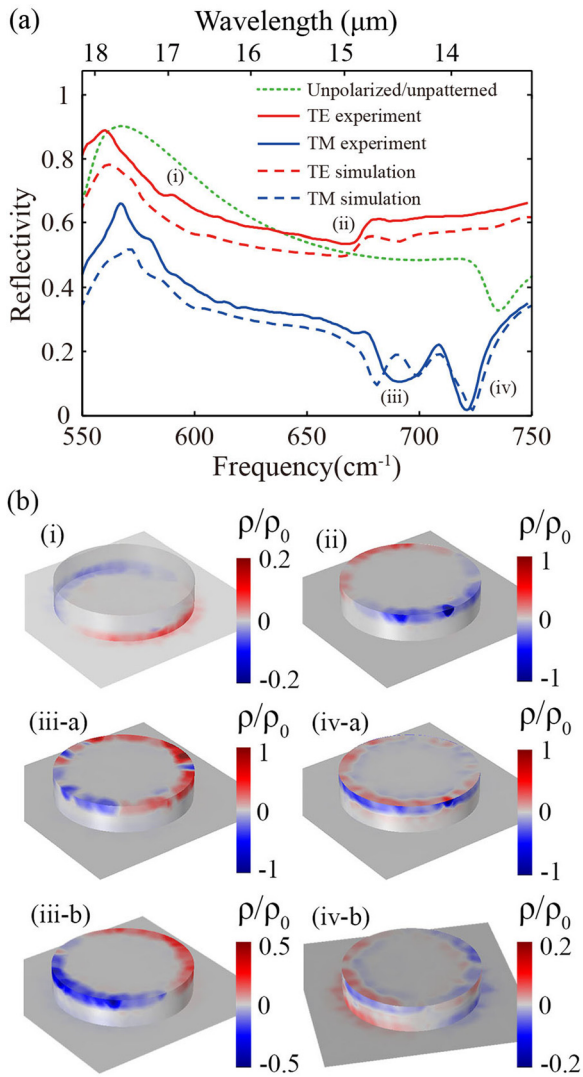

FIG. 4. (a) Experiment and simulation results of the reflection of the micro-puck array, with 45° incident angle. Light with different polarization was used. The green dotted line is the reflectance of unpatterned GaN film as a reference; the incident light is unpolarized with 40° incident angle. (b) Plots of normalized charge density of four different oscillation modes observed in 3D simulation. Unless specified, all incident angles are 45°. (i) transverse dipole (TD) for TE light at 603 cm^{-1}; (ii) TD for TE light at 673 cm^{-1}; (iii-a) charge distribution for TM light at 683 cm^{-1}; this mode is corresponding to the left one in the doublet shown in Figure 4(a); (iii-b) TD for TM light at normal incidence, 683 cm^{-1}; (iv-a) hybrid mode for TM light at 721 cm^{-1}; and (iv-b) combination of quadrupole and TD for TM light at normal incidence, 714 cm^{-1}.

polarized light has a vertical component of the electric field that also influences the charge density and electric field profiles. In Figure 4(b) (iii-a) and (iv-a) show the charge density for TM light incident at 45°; identification of the modes is complicated by the large angle of incidence. Calculations of the charge density for normal incidence for the same modes are shown in Fig. 4(b) (iii-b) and (iv-b). At normal incidence, mode (iii) is a transverse dipole mode similar to (ii), whereas at 45°, the dipolar symmetry in the charge density is altered by the vertical component of the electric field. Mode (iv) at normal incidence is a combination of a quadrupole[38] and a transverse dipole on the top and bottom of the puck, respectively. Similarly, increasing the incident angle distorts the charge distribution. In both cases, the substantial vertical component of the electric field in the incident light introduces a longitudinal dipole component and a circular charge density profile on the top of the puck begins to dominate.

In sum, we simulated, fabricated and characterized GaN based micro-puck arrays in the mid-IR portion of the spectrum. Localized SPhP modes were observed in polarization- and angle-dependent reflection measurement. The localized SPhP modes were verified and analyzed using finite different calculations. Future work includes incorporating intersubband transitions into localized geometries and rapidly controlling localized SPhPs.

The authors acknowledge funding from NSF ECCS-1420176 (A.H. and K.F.) and NSF ECCS-1420952 (D.W. and W.S.).

[1]W. L. Barnes, A. Dereux, and T. W. Ebbesen, Nature **424**, 824 (2003).
[2]V. M. Shalaev, Nat. Photonics **1**, 41 (2007).
[3]M. Kauranen and A. Zayats, Nat. Photonics **6**, 737 (2012).
[4]E. Ozbay, Science **311**, 189 (2006).
[5]A. Brolo, Nat. Photonics **6**, 709 (2012).
[6]A. Boltasseva and H. A. Atwater, Science **331**, 290 (2011).
[7]F. Stietz, J. Bosbach, T. Wenzel, T. Vartanyan, A. Goldmann, and F. Träger, Phys. Rev. Lett. **84**, 5644 (2000).
[8]S. Law, L. Yu, and D. Wasserman, J. Vac. Sci. Technol. B **31**, 03C121 (2013).
[9]S. Law, L. Yu, A. Rosenberg, and D. Wasserman, Nano Lett. **13**, 4569 (2013).
[10]J. L. Oudar, A. Migus, D. Hulin, G. Grillon, J. Etchepare, and A. Antonetti, Phys. Rev. Lett. **53**, 384 (1984).
[11]G. V. Naik, J. Kim, and A. Boltasseva, Opt. Mater. Express **1**, 1090 (2011).
[12]S. Xiao, V. P. Drachev, A. V. Kildishev, X. Ni, U. K. Chettiar, H. Yuan, and V. M. Shalaev, Nature **466**, 735 (2010).
[13]D. N. Mirlin, "Surface phonon polaritons in dielectrics and semiconductors," in *Surface Polaritons*, edited by V. M. Agranovich and D. L. Mills (North-Holland, New York, 1982), p. 3.
[14]J. D. Caldwell, A. V. Kretinin, Y. Chen, V. Giannini, M. M. Fogler, Y. Francescato, C. T. Ellis, J. G. Tischler, C. R. Woods, A. J. Giles *et al.*, Nat. Commun. **5**, 5221 (2014).
[15]S. Dai, Z. Fei, Q. Ma, A. S. Rodin, M. Wagner, A. S. McLeod, M. K. Liu, W. Gannett, W. Regan, K. Watanabe *et al.*, Science **343**, 1125 (2014).
[16]J. Watanabe, K. Uchinokura, and T. Sekine, Phys. Rev. B **40**, 5677 (1989).
[17]R. Hillenbrand, T. Taubner, and F. Keilmann, Nature **418**, 159 (2002).
[18]J. J. Greffet, R. Carminati, K. Joulain, J. P. Mulet, S. Mainguy, and Y. Chen, Nature **416**, 61 (2002).
[19]Y. Chen, Y. Francescato, J. D. Caldwell, V. Giannini, T. W. W. Mab, O. J. Glembocki, F. J. Bezares, T. Taubner, R. Kasica, M. Hong, and S. A. Maier, ACS Photon. **1**, 718 (2014).
[20]C. F. Bohren and D. R. Huffman, *Absorption and Scattering of Light by Small Particles* (John Wiley & Sons, Inc., Weinheim, Germany, 2004), p. 331.
[21]J. D. Caldwell, O. J. Glembocki, Y. Fracescato, N. Sharac, V. Giannini, F. J. Bezares, J. P. Long, J. C. Owrutsky, I. Vurgaftman, J. G. Tischyler *et al.*, Nano Lett. **13**, 3690 (2013).
[22]T. Wang, P. Li, B. Hauer, D. N. Chigrin, and T. Taubner, Nano Lett. **13**, 5051 (2013).
[23]F. Wang and Y. R. Shen, Phys. Rev. Lett. **97**, 206806 (2006).
[24]S. J. Pearton, F. Ren, A. P. Zhang, and K. P. Lee, Mater. Sci. Eng. R **30**, 55 (2000).
[25]S. J. Pearton, J. C. Zolper, R. J. Shul, and F. Ren, J. Appl. Phys. **86**, 1 (1999).
[26]A. Denis, G. Goglio, and G. Demazeau, Mater. Sci. Eng. R **50**, 167 (2006).
[27]H. Morkog and S. N. Mohammad, Science **267**, 51 (1995).
[28]M. Kubota, K. Okamoto, T. Tanaka, and H. Ohta, Appl. Phys. Express **1**, 011102 (2008).
[29]L. Liu and J. H. Edgar, Mater. Sci. Eng. R **37**, 61 (2002).
[30]F. Bernardini, V. Fiorentini, and D. Vanderbilt, Phys. Rev. B **56**, R10024(R) (1997).

[31]R. Collazo, S. Mita, A. Aleksov, R. Schlesser, and Z. Sitar, J. Cryst. Growth **287**, 586 (2006).
[32]E. T. Yu, X. Z. Dang, P. M. Asbeck, S. S. Lau, and G. J. Sullivan, J. Vac. Sci. Technol. B **17**, 1742 (1999).
[33]A. S. Barker, Jr. and M. Ilegems, Phys. Rev. B **7**, 743 (1973).
[34]J. M. Zhang, T. Ruf, M. Cardona, O. Ambacher, M. Stutzmann, J. M. Wagner, and F. Bechstedt, Phys. Rev. B **56**, 14399 (1997).
[35]H. Harima, H. Sakashita, and S. Nakashima, Mater. Sci. Forum **264–268**, 1363 (1998).
[36]H. Mutschke, A. C. Andersen, D. Clement, Th. Henning, and G. Peiter, Astron. Astrophys. **345**, 187 (1999), see http://aa.springer.de/bibs/9345001/2300187/small.htm.
[37]W. G. Spitzer, D. Kleinman, and D. Walsh, Phys. Rev. **113**, 127 (1959).
[38]F. Zhou, Z. Li, and Y. Liu, J. Phys. Chem. C **112**, 20233 (2008).